ARL-TN-1286 ● DEC 2025

Improvements to Mesoscale Tensions Test Using Laser Micromachining

by Daniel J. Magagnosc

NOTICES

Disclaimers

ARL-TN-1286 ● DEC 2025

Improvements to Mesoscale Tensions Test Using Laser Micromachining

Daniel J. Magagnosc
DEVCOM Army Research Laboratory

REPORT DOCUMENTATION PAGE

1. REPORT DATE	2. REPORT TYPE	3. DATES COVERED START DATE	END DATE
December 2025	Technical Note	2/17/2025	8/22/2025

4. TITLE AND SUBTITLE
Improvements to Mesoscale Tensions Test Using Laser Micromachining

5a. CONTRACT NUMBER	5b. GRANT NUMBER	5c. PROGRAM ELEMENT NUMBER

5d. PROJECT NUMBER	5e. TASK NUMBER	5f. WORK UNIT NUMBER

6. AUTHOR(S)
Daniel J. Magagnosc

7. PERFORMING ORGANIZATION NAME(S) AND ADDRESS(ES)
DEVCOM Army Research Laboratory
ATTN: FCDD-RLA-MB
Aberdeen Proving Ground, MD 21005

8. PERFORMING ORGANIZATION REPORT NUMBER
ARL-TN-1286

9. SPONSORING/MONITORING AGENCY NAME(S) AND ADDRESS(ES)	10. SPONSOR/MONITOR'S ACRONYM(S)	11. SPONSOR/MONITOR'S REPORT NUMBER(S)

12. DISTRIBUTION/AVAILABILITY STATEMENT
DISTRIBUTION STATEMENT A. Approved for public release: distribution unlimited.

13. SUPPLEMENTARY NOTES
ORCID: Daniel Magagnosc, 0000-0002-1418-9292

14. ABSTRACT
Use of small-scale tensile test methods is becoming prevalent in the evaluation of mechanical properties, particularly for high-throughput materials discovery. Due to the increased surface-to-volume ratio in miniaturized test specimens, sample preparation methods that produce high-quality surfaces are paramount. In this study, femtosecond laser micromachining is used to cut mesoscale tensile specimens from aluminum alloy 2024 sheets for direct comparison with conventional macroscale tests. Key bulk mechanical properties, including yield strength and ultimate tensile strength, are successfully reproduced in the mesoscale samples. The use of femtosecond laser micromachining provides high-throughput sample preparation and is the preferred fabrication method for future mesoscale testing efforts.

15. SUBJECT TERMS
mechanical testing, tensile response, subscale testing, laser micromachining, Science of Extreme Materials

16. SECURITY CLASSIFICATION OF: a. REPORT	b. ABSTRACT	C. THIS PAGE	17. LIMITATION OF ABSTRACT	18. NUMBER OF PAGES
UNCLASSIFIED	UNCLASSIFIED	UNCLASSIFIED	UU	18

19a. NAME OF RESPONSIBLE PERSON	19b. PHONE NUMBER *(Include area code)*
Daniel Magagnosc	520-691-4927

STANDARD FORM 298 (REV. 5/2020)
Prescribed by ANSI Std. Z39.18

Contents

List of Figures **iv**

List of Tables **iv**

1. Introduction **1**

2. Methods **2**

2.1 Materials 2

2.2 Macroscale Tension Testing 2

2.3 Mesoscale Tension Testing 2

2.4 Edge Roughness Measurements 3

3. Results **4**

3.1 Tensile Response 4

3.2 Machined Surface Roughness 5

4. Discussion **6**

4.1 Comparison of Macroscale and Mesoscale Tension Tests 6

4.2 Improved Mesoscale Specimen Fabrication and Testing 7

5. Conclusion **8**

6. References **9**

List of Symbols, Abbreviations, and Acronyms **11**

Distribution List **12**

List of Figures

Figure 1. Full-scale ASTM E8-24 tension bar (bottom) and an array of mesoscale tension samples (middle). A ruler (top) is included for scale. 4

Figure 2. Representative stress–strain curves for macroscale (left) and mesoscale (right) tension bars. 4

Figure 3. Optical micrographs of specimen edges prepared via a) femtosecond laser cutting, b) abrasive waterjet cutting, and c) micromilling. d) Linear surface profiles from each specimen for surface roughness measurement are included. 6

List of Tables

Table 1. Nominal composition in wt% for AA 2024 according to AMS4037R.2

Table 2. Summary of measured mechanical properties and minimum properties required by AMS4037R. 5

1. Introduction

Small-scale testing mechanical testing approaches are becoming a prevalent approach for evaluating mechanical properties.[1–3] In particular, incorporating miniaturized tension testing methods into high-throughput materials discovery is of great interest.[4] Recently, the standard test method for evaluating tensile properties in metallic materials (ASTM E8-24)[5] was updated to include provisions for miniature test specimens.

Several well-known phenomena affect the measured tensile response of a material when reducing length scales. Flaw-dominated materials such as ceramics exhibit well-documented size effects leading to increased tensile strengths as size decreases.[6,7] Material behavior also becomes increasingly stochastic as the test article size approaches the length scale of critical microstructural features.[8]

Beyond materials-specific factors, care must be taken during sample fabrication to avoid altering the tensile response. As specimen length scale decreases, surface effects increasingly dominate; the surface-to-volume ratio scales as approximately 1/m. The increasing dominance of surface effects in small specimens impacts the choice of sample fabrication route. Conventional processes, such as mechanical machining and electrical discharge machining (EDM), have microscale analogs.[9,10] However, producing high-quality, defect-free surfaces become increasingly challenging as critical features sizes decrease.

Femtosecond laser micromachining is an increasingly viable fabrication method to produce miniaturized test specimens.[11–13] By varying the laser spot size, power, and repetition rate, a wide range of material removal rates and critical dimensions can be achieved. These capabilities bridge the size regimes of micromilling and micro EDM with nanoscale fabrication approaches such focused ion beam machining.[14–16] In addition, femtosecond laser ablation introduces a minimal heat-affected zone, often on the order of a few microns, thereby preserving the materials microstructure.[17]

In this report, the efficacy of femtosecond laser micromachining for fabricating tensile test specimens is demonstrated. Macroscale tension bars are directly compared with mesoscale samples produced via laser machining. The extracted mechanical properties are consistent regardless of specimen size, which represents a significant improvement over prior mesoscale testing. As a result, femtosecond laser micromachining is demonstrated as an enabling technology for high-throughput evaluation of mechanical properties.

2. Methods

2.1 Materials

Aluminum alloy (AA) 2024 was obtained in the T3 temper (cold worked and naturally aged) in 0.508-mm-thick sheets. The sheets were produced in accordance with AMS4037R.[18] The nominal composition is listed in Table 1.

Table 1. Nominal composition in wt% for AA 2024 according to AMS4037R.[18]

Element	Minimum	Maximum
Copper	3.8	4.9
Magnesium	1.2	1.8
Manganese	0.3	0.9
Silicon	. . .	0.5
Iron	. . .	0.5
Zinc	. . .	0.25
Titanium	. . .	0.15
Chromium	. . .	0.1
Aluminum	Balance	

2.2 Macroscale Tension Testing

Macroscale tensile specimens were cut using a WAZER Desktop abrasive waterjet parallel to the rolling direction. The samples were cut using an abrasive feed rage of 0.15 kg/min and a cutting feed rate of 148 mm/min. The sample geometry followed ASTM E8-24[5] standard size specimen for sheet materials. Nominal dimensions of the uniform gage section were 50 mm long, 12.7 mm wide, and 0.508 mm thick. After cutting, the specimens were buffed on a Scotch-Brite belt to remove edge burrs.

Macroscale tension tests were performed using an Instron 5984 electromechanical universal testing system equipped with a 10-kN load cell. Tests were conducted at a nominal strain rate of 10^{-3} s^{-1} with an applied crosshead velocity of 0.05 mm/s. Strains were determined using 3D digital image correlation (DIC). The specimens were painted with a white base coat and speckled with black spray paint. The strains were then calculated using the Vic3D software.

2.3 Mesoscale Tension Testing

Mesoscale samples were produced using a multi-axis femtosecond laser machining system. The cutting laser was generated using a Clark-MXR Impulse HE fiber laser operating at a 200-kHz repetition rate, an emission wavelength of 1030 nm, and a pulse duration less than 250 fs. The fiber laser output was frequency doubled in a second harmonic generator resulting in a 515-nm working beam; the average power was controlled using a rotating wave plate between 1 and 2 W. Finally, the laser was focused using an F-theta lens with a 150-mm focal length. This enables the beam to be positioned using a two-axis galvanometer with a nominal field of view of 30 × 30 mm. The laser was integrated with a five-axis motion system, consisting of x, y, and z axes position stages as well as tilt and rotation axes. The five-axis motion system, in combination with the fast-scanning galvanometer, enables precision machining across large areas.

Mesoscale tension specimens were laser cut parallel to the rolling direction. The sample geometry was consistent with recommendations in ASTM E8-24[5] A1 Miniature Specimens. The nominal gage dimensions were 4 mm long, 1 mm wide, and 0.508 mm thick. The mesoscale samples were cut in a two-step process. First, the sample profile is cut at normal incidence at an average power of 1.6 W until the material is fully perforated. Second, the sample is tilted using the integrated tilt axis to 5°; the edge profile is cut again to remove the taper produced during the first cut. The finish passes are executed with an average laser power of 1.2 W. All laser cuts were performed at a feed rate of 100 mm/s.

Mesoscale specimen dimensions were measured optically using a Keyence VHX7000 digital microscope. Tensions tests were performed using a Psylotech µTS universal load frame equipped with a 1.6-kN load cell and integrated optical microscope. Tests were performed at a nominal strain rate 10^{-3} s^{-1} with an applied crosshead velocity of 40 µm/s. Strains were calculated from optical microscope images using 2D DIC. The samples were speckled with black toner powder after applying a white base coat. The strains were calculated using Vic2D.

2.4 Edge Roughness Measurements

The edge quality of the femtosecond laser and abrasive waterjet cut samples was assessed via linear surface roughness. The surface quality of the laser and waterjet cut samples is compared with that of a micro-milled sample. Details on micromilling sample preparation are found in Wagner and Yin.[19] Optical micrographs of the edges were captured on a Keyence VHX7000 digital microscope. Surface roughness was measured via an Olympus OLS5100 laser scanning microscope. Height line profiles were collected using a 100× objective over a total line length of 3 mm. The resulting line profiles were flattened, and linear roughness was measured.

3. Results

3.1 Tensile Response

An example of a full-scale ASTM E8-24[5] tension bar and an array of 12-fs laser cut specimens is illustrated in Figure 1. This shows the significant savings of material using the femtosecond laser; the total cutting time for a mesoscale specimen was approximately 20 min.

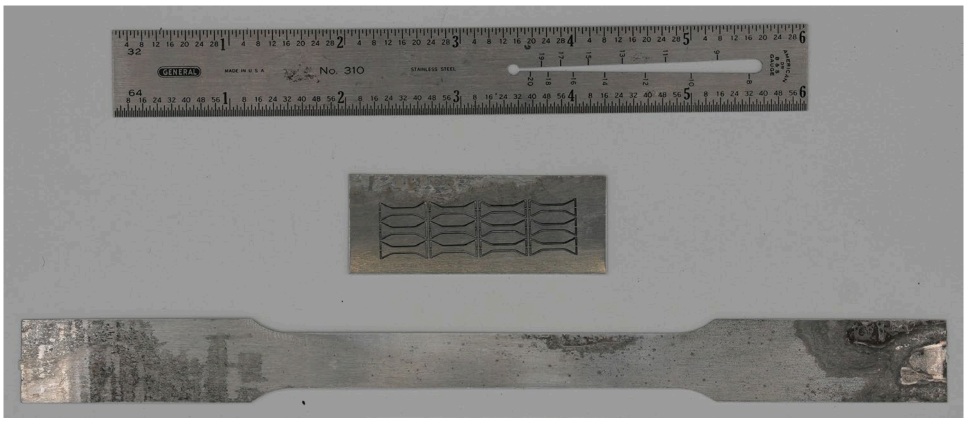

Figure 1. Full-scale ASTM E8-24[5] tension bar (bottom) and an array of mesoscale tension samples (middle). A ruler (top) is included for scale.

Figure 2 presents the stress–strain response for both the macroscale and mesoscale tensile samples. The stress–strain response is a similar shape regardless of the specimen size; all curves show linear elastic behavior up to the yield point, followed by strain hardening until the ultimate tensile stress (UTS). In the macroscale samples, failure occurs soon after the UTS, whereas the mesoscale samples exhibit some post-necking ductility.

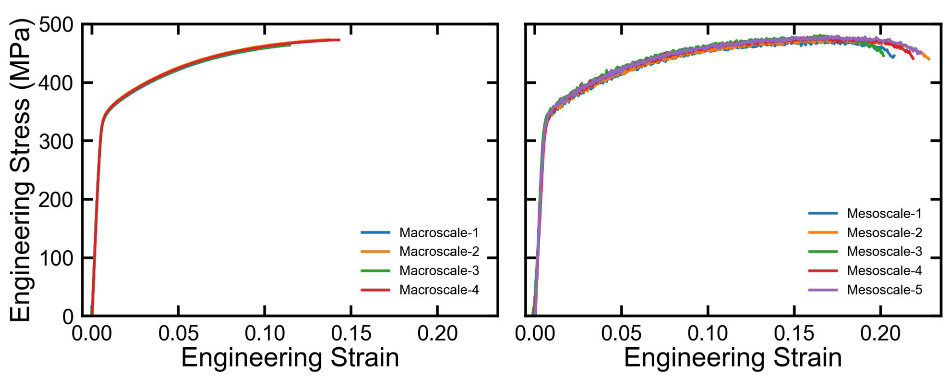

Figure 2. Representative stress–strain curves for macroscale (left) and mesoscale (right) tension bars.

The average mechanical properties are summarized in Table 2 and compared with the minimum property requirements per AMS4037R.[18] The macroscale and mesoscale properties show excellent agreement. Both samples have comparable elastic modulus values with the mesoscale sample showing greater scatter. For both sample geometries, the measured elastic modulus is lower than expected. This discrepancy is typical of elastic moduli measured during initial tensile loading.

Table 2. Summary of measured mechanical properties and minimum properties required by AMS4037R.[18]

Sample	Young's modulus (GPa)	Yield strength (MPa)	UTS (MPa)	% elongation
Macroscale	66.8 ± 0.2	338 ± 1	469 ± 5	13.3 ± 3.6
Mesoscale	64.4 ± 4	337 ± 5	477 ± 3	21.7 ± 1
AMS4037R	. . .	290	434	12

The yield strengths for both specimen sizes are within the measurement error. For the mesoscale sample, the UTS increases slightly while the total elongation is significantly increased. Both macroscale and mesoscale samples exceed the minimum specification for AA 2024-T3 sheet.

3.2 Machined Surface Roughness

Optical micrographs collected from the edge of a femtosecond laser cut, abrasive waterjet cut, and micro-milled specimen are shown in Figures 3a–c. The femtosecond laser cut surface shows fine-scale serrations with spacing on the order of the laser spot size (e.g., 20 µm). The waterjet cut surface exhibits a randomly textured surface with no obvious repeating features. Finally, the milled surface exhibits a periodic trough pattern with the trough features extending through the thickness. The periodic features are approximately 100 µm wide.

Linear roughness was measured from laser scanning microscope line profiles collected from the edges of each sample. The line profiles were collected at approximately one-half the sheet thickness parallel to the sample surface and are shown in Figure 3d. From the height profile, the average linear roughness (Ra) was determined to be 1.68, 5.60, and 1.18 µm for the femtosecond laser cut, abrasive waterjet cut, and micro-milled specimens, respectively.

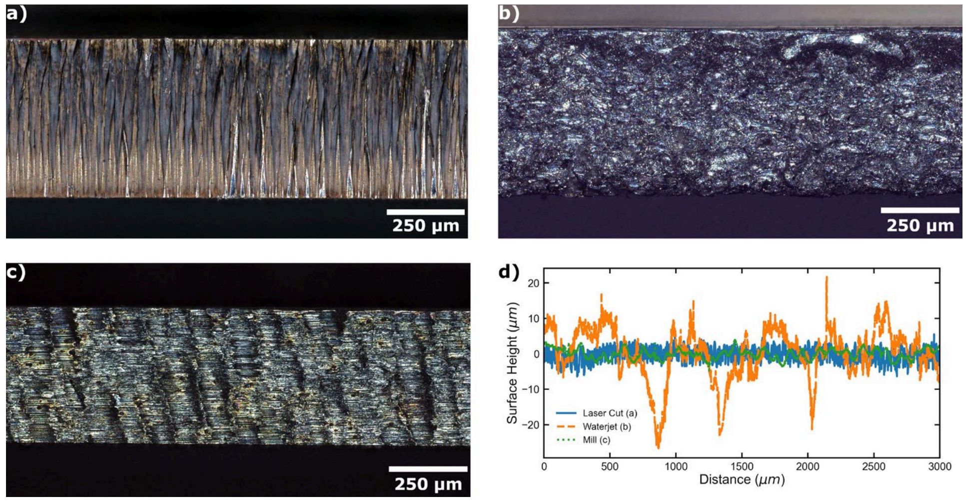

Figure 3. Optical micrographs of specimen edges prepared via a) femtosecond laser cutting, b) abrasive waterjet cutting, and c) micromilling. d) Linear surface profiles from each specimen for surface roughness measurement are included.

4. Discussion

4.1 Comparison of Macroscale and Mesoscale Tension Tests

Using femtosecond laser micromachining to cut miniaturized tensile specimens resulted in mechanical property measurements that are comparable with conventional ASTM E8-24[5] tension samples. Although the measured elastic modulus for the mesoscale samples is lower than that of the macroscale samples, the elastic modulus for the macroscale samples is within the experimental spread for the mesoscale samples; the yield strengths for the two sample geometries are identical.

In contrast, the UTS and total elongation are higher for the mesoscale sample. The increased UTS in the laser cut specimens is attributable to the greater strains. The uniform elongation (16.9% ± 0.7%) in the mesoscale sample exceeds the total elongation of the macroscale sample (13.3% ± 3.6%). Consequently, the mesoscale samples exhibit greater strain hardening than the macroscale samples. Alternatively, the average flow stress in the mesoscale samples at the average maximum strain for the full-scale specimens can be compared with the full-scale UTS. Here, the average flow stress for the laser cut samples at 13.3% strain is 469 ± 3 MPa, which is identical to the UTS of the macroscale samples.

The greater elongation in the laser cut specimens is attributed to the improved surface quality in the laser cut samples. Abrasive waterjet cutting produced a surface with a 5.60-µm Ra. In addition, numerous large valleys are observed on the edge of the macroscale specimens. These valleys are likely to serve as initiation sites for necking and fracture. In contrast, femtosecond laser machining produced a more uniform surface with much lower roughness (1.68-μm Ra); no large valleys are observed on the laser cut surface. Femtosecond laser machining is also well documented to produce minimal subsurface microstructural damage. Absent any initiation sites, the laser cut mesoscale samples deform to a greater extent than the macroscale samples.

4.2 Improved Mesoscale Specimen Fabrication and Testing

Improved tension test fixturing and sample fabrication represent a significant improvement over prior reports on mesoscale mechanical testing.[20] In the previous work on ultra-high strength steels (UHSS), mesoscale samples reproduced the general behavior of full-scale tension samples. However, the yield strength and UTS were consistently overestimated while total elongation was reduced. These discrepancies across length scales were attributed to sample alignment within the load frame, notch-strengthening effects, and surface damage layers. The improved test fixtures and sample fabrication specifically address these issues as follows.

New gripping fixtures were acquired to aid in sample alignment. The new fixtures are adapted from the mesoscale test frames manufacture's full-scale tension dog bone geometry and require no manual alignment. Use of these grips has significantly reduced settling of the sample and the resulting nonlinear behavior at the onset of loading. Although a foot correction is still performed for the mesoscale tests, the magnitude of the correction is reduced by a factor of three relative to prior reports.[20]

Previous samples were produced via micromilling. Micromilling can produce high-quality surfaces (see Figure 3) and is amenable to rapid sample fabrication. However, consistently obtaining high-quality surfaces requires optimizing many machining parameters, rigid feedstock fixturing, and managing tool life, all of which are processes that can vary significantly between materials.[9] As shown previously, notch strengthening and surface damage was observed to impact the measured UTS and total elongation in micro-milled UHSS samples.[20]

In contrast, the use of femtosecond laser cutting provides a reliable, high-throughput approach for sample fabrication. As shown in Figure 3, femtosecond laser cutting produces uniform, fine-scale surface structures and low average roughness. Absent the presence of significant stress concentrators such as notches, the bulk UTS and elongation behavior is reproduced (Figure 2). Furthermore, the limited surface damage induced by the femtosecond laser ablation process, typically less than 1 μm,[13,17] results in very similar yield strengths and flow stresses compared with macroscale samples (Table 1).

Another advantage of femtosecond laser cutting is the minimal setup or optimization of the cutting process. Ablation thresholds, the primary materials parameter affecting the cutting process, do not vary significantly among metals or even across materials classes.[21–23] Consequently, few parameters must be tuned to obtain high-quality specimens. Furthermore, fiber laser output power is highly stable with less than 1% root mean square variation per the manufacturer's specification. As a result, femtosecond laser cutting is the preferred approach for mesoscale sample fabrication.

5. Conclusion

Femtosecond laser micromachining has been demonstrated as a viable method for producing mesoscale tension testing specimens. Compared with macroscale tests, the mesoscale tests yield comparable values for elastic modulus, yield strength, and ultimate tensile strength. Greater strains to failure were observed in the mesoscale samples.

The use of femtosecond laser micromachining represents an improvement over previous mesoscale testing efforts. The improvements are attributed to high-quality surface finishes obtained via laser machining compared with abrasive waterjet cutting or micromilling. The elimination of stress concentrations and subsurface damage mitigates potential notch-strengthening effects, delays localization, and provides reliable yield strengths. For future mesoscale testing studies, femtosecond laser micromachining is the preferred sample fabrication method due to its adaptability to many materials systems.

6. References

1. Gianola DS et al. Advances and opportunities in high-throughput small-scale mechanical testing. Curr Opin Solid State Mater Sci. 2023;27(4):101090.

2. Sharpe WN. Murray lecture tensile testing at the micrometer scale: opportunities in experimental mechanics. Exp Mech. 2003;43(3):228–237.

3. Hemker KJ, Sharpe WN. Microscale characterization of mechanical properties. Ann Rev Mater Res. 2007;37:93–126.

4. Heckman NM et al. Automated high-throughput tensile testing reveals stochastic process parameter sensitivity. Mater Sci Eng A. 2020;772:138632.

5. ASTM E8-24. Standard test methods for tension testing of metallic materials. ASTM International; 2024.

6. Magagnosc DJ, Schuster BE. Fracture strength of hot-pressed silicon carbide at the microscale. Mater Sci Eng A. 2019;765:138297.

7. Lu C, Danzer R, Fischer FD. Scaling of fracture strength in ZnO: effects of pore/grain-size interaction and porosity. J Euro Ceram Soc. 2004;24(14):3643–3651.

8. Echlin MP, Lenthe WC, Pollock TM. Three-dimensional sampling of material structure for property modeling and design. Integrat Mater Manuf Innov. 2014;3(1):278–291.

9. Dornfeld D, Min S, Takeuchi Y. Recent advances in mechanical micromachining. CIRP Ann. 2006;55(2):745–768.

10. Mahendran S, Devarajan R, Nagarajan T, Majd A. A review of micro-EDM. Proceedings of the International MultiConference of Engineers and Computer Scientists; 2010 Mar 12–19; Hong Kong.

11. Lei S et al. Ultrafast laser applications in manufacturing processes: a state-of-the-art review. J Manuf Sci Eng. 2020;142(3):031005.

12. Magagnosc DJ, Ligda JP, Sano T, Schuster BE. Femtosecond laser machining of micro-tensile specimens for high throughput mechanical testing. In: Starman L, Hay J, editors. Springer International Publishing; 2018. p. 7–9. (Micro and nanomechanics; vol. 5).

13. Pfeifenberger MJ et al. The use of femtosecond laser ablation as a novel tool for rapid micro-mechanical sample preparation. Mater Des. 2017;121:109–118.

14. Calabrese L et al. Micro-milling process of metals: a comparison between femtosecond laser and EDM techniques. J Manuf Mater Process. 2021;5(4):125.

15. Volkert CA, Minor AM. Focused ion beam microscopy and micromachining. MRS Bull. 2011;32(05):389–399.

16. Smith NS et al. High brightness inductively coupled plasma source for high current focused ion beam applications. J Vac Sci Technol B. 2006;24(6):2902.

17. Echlin MP, Titus MS, Straw M, Gumbsch P, Pollock TM. Materials response to glancing incidence femtosecond laser ablation. Acta Mater. 2017;124: 37–46.

18. AMS4037R. Aluminum alloy, sheet and plate 4.4Cu - 1.5Mg - 0.60Mn (2024; -T3 flat sheet, -T351 plate) solution heat treated. SAE International; 2020.

19. Wagner T, Yin D. Development of subscale tester for high-cycle fatigue evaluation. DEVCOM Army Research Laboratory (US); 2022. Report No.: ARL-TR-9378.

20. Magagnosc DJ, Rupinen MC, Field DM. Evaluation of mesoscale tension tests for rapid screening of mechanical properties in high-strength steels. DEVCOM Army Research Laboratory (US); 2025. Report No.: ARL-TN-1215.

21. Chichkov BN, Momma C, Nolte S, Alvensleben F, Tünnermann A. Femtosecond, picosecond and nanosecond laser ablation of solids. Appl Phys A. 1996;63(2):109–115.

22. Shaheen ME, Gagnon JE, Fryer BJ. Femtosecond laser ablation behavior of gold, crystalline silicon, and fused silica: a comparative study. Laser Phys. 2014;24(10):106102.

23. Gamaly EG, Rode AV, Luther-Davies B, Tikhonchuk VT. Ablation of solids by femtosecond lasers: ablation mechanism and ablation thresholds for metals and dielectrics. Phys Plasmas. 2002;9(3):949.

List of Symbols, Abbreviations, and Acronyms

2/3D	two-/three-dimensional
AA	aluminum alloy
ASTM	American Society for Testing and Materials
DIC	digital image correlation
EDM	electrical discharge machining
Ra	average linear roughness
UHSS	ultra-high strength steel
UTS	ultimate tensile stress

1 (PDF)	DEFENSE TECHNICAL INFORMATION CTR DTIC OCA
1 (PDF)	DEVCOM ARL FCDD RLB CI TECH LIB